JCTC Journal of Chemical Theory and Computation

Article

pubs.acs.org/JCTC

Magnetization Dynamics from Time-Dependent Noncollinear Spin Density Functional Theory Calculations

Juan E. Peralta,*[,†] Oded Hod,[‡] and Gustavo E. Scuseria[¶,§]

[†]Department of Physics, Central Michigan University, Mt. Pleasant, Michigan 48859, United States

[‡]Department of Chemical Physics, School of Chemistry, Raymond and Beverly Sackler Faculty of Exact Sciences, Tel Aviv University, Tel Aviv 6997801, Israel

[¶]Department of Chemistry and [§]Department of Physics and Astronomy, Rice University, Houston, Texas 77005, United States

Supporting Information

ABSTRACT: A computational scheme, based on a time-dependent extension of noncollinear spin density functional theory, for the simultaneous simulation of charge and magnetization dynamics in molecular systems is presented. We employ a second-order Magnus propagator combined with an efficient predictor-corrector scheme that allows us to treat large molecular systems over long simulation periods. The method is benchmarked against the low-frequency dynamics of the H−He−H molecule where the magnetization dynamics can be modeled by the simple classical magnetization precession of a Heisenberg−Dirac-van Vleck Hamiltonian. Furthermore, the magnetic exchange couplings of the bimetallic complex $[Cu(bpy)(H_2O)(NO_3)_2(\mu\text{-}C_2O_4)]$ (BISDOW) are extracted from its low-frequency spin precession dynamics showing good agreement with the coupling obtained from ground state energy differences. Our approach opens the possibility to perform real-time simulation of spin-related phenomena using time-dependent density functional theory in realistic molecular systems.

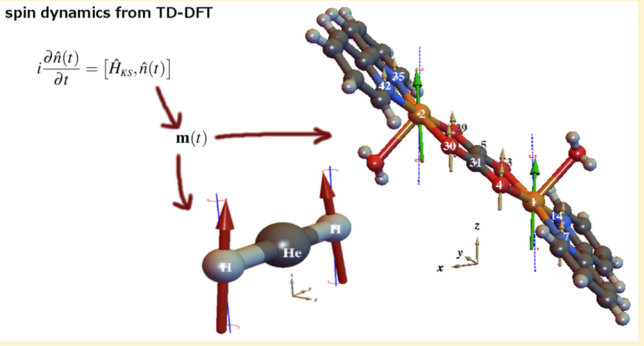

1. INTRODUCTION

Time-dependent density functional theory (TDDFT) provides an efficient theoretical framework for the evaluation of excited-state properties in molecules and extended systems where wave function based methods are computationally unaffordable.[1−4] Advanced computational methods based on TDDFT either in the linear-response regime or via explicit time-evolution are becoming the tool of choice for tackling a variety of problems in the fields of chemistry, biology, and materials science.[3,5] In particular, numerical simulations based on explicit time-evolution have been utilized to calculate nonlinear optical absorption spectra in molecular systems,[6−9] charge transfer dynamics in biomolecules,[10,11] excited state electron dynamics in extended systems,[5] cluster dynamics under strong laser fields,[12] as well as the simulation of time-dependent phenomena in molecular conductance.[13−17] In most cases, computational schemes focus on spin-compensated systems and employ the same exchange-correlation kernel as ground-state DFT (adiabatic approximation) to determine the time-dependent electronic charge density $n(t)$. These schemes are based on numerical integration of the equations of motion for the time evolution of the occupied Kohn−Sham (KS) orbitals (atomic units will be used herein)

$$i\frac{\partial\psi_k(t)}{\partial t} = \hat{H}_{KS}\psi_k(t) \tag{1}$$

or equivalently integrating the Liouville-von Neumann equation for the charge density $n(t)$

$$i\frac{\partial\hat{n}(t)}{\partial t} = [\hat{H}_{KS}, \hat{n}(t)] \tag{2}$$

where $\hat{H}_{KS}$ is the KS Hamiltonian and $n(t) = \langle\hat{n}(t)\rangle$ is expanded in terms of $\psi_k(t)$ as in standard KS theory. Despite the success of these schemes, much less attention has been given to the dynamics of the spin degrees of freedom that are responsible for a wealth of important chemical and physical phenomena.[18−20] It should be pointed out that including the spin-density in TDDFT simulations in the most general form necessarily implies dealing with noncollinear magnetization to properly account for both, $n(t)$ and the magnetization density vector $\mathbf{m}(t)$ (see Section 2.2 for a detailed definition).[21,22]

Noncollinear magnetization has been introduced in DFT to model systems where the spin density adopts noncollinear structures, such as helical spin density waves or spin spirals for the ground state of γ-Fe,[23,24] geometrically frustrated systems like, for instance, the Kagomé antiferromagnetic lattice,[25] and systems with competing magnetic interactions, such as the composite magnets $LaMn_2Ge_2$[26] and $Fe_{0.5}Co_{0.5}Si$.[27] In these

Received: May 26, 2015
Published: July 7, 2015

DOI: 10.1021/acs.jctc.5b00494
J. Chem. Theory Comput. 2015, 11, 3661−3668

cases noncollinear spin structures arise from the solutions of the (time-independent) KS equations with 2-component spinors. These 2-component KS equations require a noncollinear XC kernel. Developments of XC approximations for noncollinear magnetization were early based on extensions of the LSDA approximation,[28−30] and later based on the generalized gradient approximation (GGA) and meta-GGA.[29,31−33] For excited-states, noncollinear magnetization has been employed in the linear-response formalism for the evaluation of spin-flip type excitations.[34−36] Beyond the linear-response regime, a time-evolution scheme that involves noncollinear magnetization dynamics has been proposed in the framework of Hartree−Fock theory and for the adiabatic LSDA in a basis-free real-space representation,[37,38] as well as in an all electron solid-state code based on plane-waves.[39]

The purpose of this paper is to present a computational method for the simultaneous time propagation of charge and spin density in molecular systems within the noncollinear spin TDDFT formalism that provides the most general description of excited state magnetization dynamics. We base our approach on an atomic-centered Gaussian basis-set representation that is highly suitable for performing calculations on molecular systems.[40] This allows us to efficiently follow the spin dynamics in realistic molecular complexes over long simulation periods. Particularly, we demonstrate the method on two model systems: (i) a simple two-center HeH_2 molecule and (ii) the $[Cu(bpy)(H_2O)(NO_3)2(\mu\text{-}C_2O_4)]$ bimetallic complex. For both systems we study the low-frequency magnetization precession at the magnetic centers and extract the corresponding magnetic exchange couplings.

2. METHODOLOGY

Two-component KS complex spinors are employed to calculate the density and spin-density in analogy to the ground-state case. These KS spinors can be expressed as

$$\Psi_i(\mathbf{r}, t) = \begin{pmatrix} \psi_i^{\alpha}(\mathbf{r}, t) \\ \psi_i^{\beta}(\mathbf{r}, t) \end{pmatrix} \tag{3}$$

where $\psi_i^{\sigma}(\mathbf{r},t)$ are spatial molecular orbitals expanded as a linear combination of (time-independent) standard atomic orbitals (AO) $\phi_\mu(\mathbf{r})$:

$$\psi_i^{\sigma}(\mathbf{r}, t) = \sum_{\mu} c_{\mu i}^{\sigma}(t)\phi_\mu(\mathbf{r}) \quad (\sigma = \alpha, \beta) \tag{4}$$

Note that the two-component spinors $\Psi_i(t)$ are not necessarily eigenfunctions of any component of the spin operator. In eq 4, the time-dependence of ψ_i^{α} and ψ_i^{β} has been made explicitly through the coefficients $c_{\mu i}^{\sigma}$. From these coefficients, the one-particle density matrix $\mathbf{D}$ can be expressed as

$$D_{\mu\nu}^{\sigma\sigma'}(t) = \sum_{i\in occ} c_{\mu i}^{\sigma}(t)c_{\nu i}^{\sigma'*}(t) \tag{5}$$

2.1. Time-Evolution. In our implementation, we consider the time-evolution of the KS system as given by the Liouville-von Neumann equation for the one-particle density matrix $\mathbf{D}$ of eq 5 in the generally nonorthogonal AO basis

$$i\mathbf{S}\frac{\partial \mathbf{D}}{\partial t}\mathbf{S} = \mathbf{H}_{KS}\mathbf{D}\mathbf{S} - \mathbf{S}\mathbf{D}\mathbf{H}_{KS} \tag{6}$$

where $\mathbf{S}$ is the (real) AO overlap matrix, and the KS Hamiltonian $\mathbf{H}_{KS}$ depends implicitly on t through $\psi_i^{\alpha}(\mathbf{r},t)$ and $\psi_i^{\beta}(\mathbf{r},t)$, and possibly explicitly through terms including for instance memory kernels[41−43] and time-dependent electromagnetic fields. Following ref 21, $\mathbf{H}_{KS}$ can be cast as

$$\mathbf{H}_{KS} = (\mathbf{T} + \mathbf{V}_E + \mathbf{J} + \mathbf{V}_{XC}) \tag{7}$$

where on the right-hand side of eq 7 are the matrix representation of the (nonrelativistic) kinetic energy operator $\mathbf{T}$, the external potential (including the nuclei-electron interaction, and possibly external magnetic or electric fields) $\mathbf{V}_E$, the electron−electron Coulomb interaction $\mathbf{J}$, and the exchange-correlation (XC) potential $\mathbf{V}_{XC}$, which contains a scalar and a magnetic vector components (described in Section 2.2).

Time propagation is carried out using a standard second-order Magnus expansion.[44,45] In short, starting from the density matrix at time t, $\mathbf{D}(t)$, the time-evolved density $\mathbf{D}(t+dt)$ is given by

$$\mathbf{D}(t + dt) = \mathbf{U}(t + dt, t)\mathbf{D}(t)\mathbf{U}(t + dt, t) \tag{8}$$

where $\mathbf{U}(t+dt,t)$ is the time-propagation matrix that is approximated by

$$\mathbf{U}(t + dt, t) \approx \exp[-i\mathbf{H}_{KS}(t + dt/2)dt] \tag{9}$$

Here, the half-step KS Hamiltonian $\mathbf{H}_{KS}(t+dt/2)$ is extrapolated using the second-order predictor-corrector scheme proposed by Cheng et al.[46] This strategy has been proven to provide reasonable accuracy and stability at moderate computational cost for the type of simulations performed in this study.[47] The matrix exponential in eq 9 is evaluated using the "scaling and squaring" algorithm with Taylor expansion.[48] This algorithm has been reported to be one of the most efficient and stable alternatives for the exponential of a matrix, effectively reducing the numerical error and computational cost associated with the known problem of overcoming the "hump".[48] It should be noted that the main two differences between a spin-compensated and our noncollinear time-propagation algorithm are the dimension of the matrices (they are doubled in our case) and the formation of $\mathbf{H}_{KS}$. For the collinear (spin unrestricted) case,[49] on the other hand, the time-propagation involves only the two same-spin diagonal KS Hamiltonian blocks and therefore the dimension of the matrices and the formation of $\mathbf{H}_{KS}$ is similar to that of the standard spin-unrestricted case.

2.2. Noncollinear Spin DFT. The methodology presented in Section 2.1 is of general nature and can be applied in conjunction with any density functional approximation, including meta-GGAs and hybrid functionals, provided that there is a prescription for the construction of V_{XC}. For simplicity, and in favor of conciseness, in this work we focus on density functionals of the GGA family. The most general form of a noncollinear GGA XC energy functional depends on the magnetization $\mathbf{m}(\mathbf{r}) = \sum_{i\in occ}\Psi_i^{\dagger}(\mathbf{r})\boldsymbol{\sigma}\Psi_i(\mathbf{r})$ and its gradients $\nabla\mathbf{m}(\mathbf{r})$, where $\boldsymbol{\sigma}$ are the Pauli matrices.[21] A straightforward approach to obtain approximate functionals for the noncollinear magnetization case that are invariant under rotations of the spin quantization axis and reduce to the spin collinear case for collinear spin densities is to heuristically replace $m_z(\mathbf{r})$ from the standard collinear case with $|\mathbf{m}(\mathbf{r})|$, and $\nabla m_z(\mathbf{r})$ with $\nabla|\mathbf{m}(\mathbf{r})|$.[32,33,50] Here, we briefly review this approach. The XC energy functional E_{XC} can be generalized to the noncollinear spin case as

DOI: 10.1021/acs.jctc.5b00494
J. Chem. Theory Comput. 2015, 11, 3661−3668

$$E_{XC} = \int d^3r f(n_+, n_-, \nabla n_+, \nabla n_-) \tag{10}$$

where the subindices + and − refer to variables expressed in a local (pointwise) reference frame along the local spin quantization axis

$$n_\pm = \frac{1}{2}(n \pm |\mathbf{m}|) \tag{11}$$

In the collinear spin case, $n = n_\alpha + n_\beta$ and $|m| = |n_\alpha - n_\beta|$, and thus n_+ and n_- become n_α and n_β, respectively. This approach provides a straightforward extension of existing collinear spin approximations by assuming that E_{XC} depends on the local variables n_+ and n_- in the same way as in the standard collinear case (where it depends on n_α and n_β). The XC potential is obtained as a functional derivative of E_{XC} with respect to n and $\mathbf{m}$. A general prescription that considers GGAs, meta-GGAs, and hybrid functionals for the noncollinear magnetization case utilized in this work is given in ref 33, where the XC potential matrix needed to construct $\mathbf{H}_{KS}$ is also derived. The XC potential can be expressed in terms of a scalar component, $V^0_{XC}(\mathbf{r})$, and a magnetic vector part, $\mathbf{B}_{XC}(\mathbf{r})$

$$V_{XC}(\mathbf{r}) = V^0_{XC}(\mathbf{r}) + \boldsymbol{\sigma}\cdot\mathbf{B}_{XC}(\mathbf{r}) \tag{12}$$

Within this approach, $\mathbf{B}_{XC}(\mathbf{r})$ is parallel to $\mathbf{m}(\mathbf{r})$ and hence the XC magnetic torque $\mathbf{B}_{XC}(\mathbf{r}) \times \mathbf{m}(\mathbf{r})$ becomes zero. Since $\mathbf{T}$, $\mathbf{V}_E$, and $\mathbf{J}$ are block-diagonal in the 2-dimensional spin space, the only term in eq 7 that couples the α and β spin components is $\mathbf{V}_{XC}$ (the spin−orbit operator is neglected in this work; however, if present it also couples the two spinor components).[51−53] This approach is not the most general possibility to define energy functionals for noncollinear magnetic systems.[21,54] Although the purpose of this work is to focus on the spin dynamics rather than exploring alternatives to extend XC functionals to the noncollinear regime, it should be mentioned that an approach that incorporates (orbital dependent) Hartree−Fock exchange using optimized effective potentials[22] and a generalization of the XC energy for the noncollinear case that improves self-consistent convergence in ground state calculations has been proposed recently.[55−57]

3. COMPUTATIONAL DETAILS

The choice of initial state and boundary conditions in dynamic simulations should reflect the external perturbations that drive the system out of equilibrium, the desired measurable property, and/or the physical and chemical processes under consideration. For example, transient electric fields have been used to simulate the action of short laser pulses[47] for spectral analysis and in photodissociation processes,[58] and charge density constraints have been applied to simulate molecular conductance.[46]

Since our purpose is to analyze the dynamics of the magnetization, we need an initial state that sets off the proper dynamics. To this end, we choose an initial state where the local spins are in a noncollinear configuration (see, e.g., Figure 1). This is implemented by applying constraints introduced via Lagrange multipliers in the same way some of us have done previously[59,60] for the static calculation of magnetic exchange couplings. Using local projectors $\mathcal{W}^A$,[61,62] we write the local magnetization at atom A as

$$\mathbf{m}_A = \sum_{\mu,\nu} \mathcal{W}^A_{\mu\nu}\mathbf{P}_{\mu\nu} \tag{13}$$

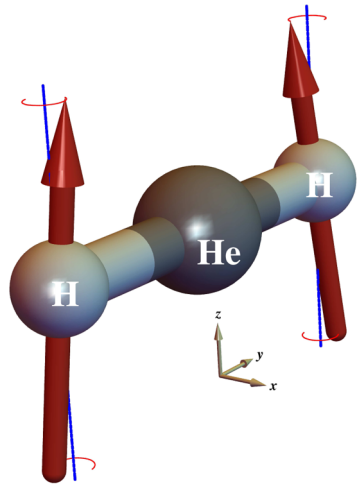

Figure 1. Representation of the magnetization precession at each H atom in the linear H−He−H molecule. The arrows represent the magnetization orientation evaluated as described in the text.

where $\mathbf{P}_{\mu\nu}$ is the spin-density matrix vector whose Cartesian components are

$$P^x_{\mu\nu} = D^{\alpha\beta}_{\mu\nu} + D^{\beta\alpha}_{\mu\nu} \tag{14}$$

$$P^y_{\mu\nu} = i(D^{\alpha\beta}_{\mu\nu} - D^{\beta\alpha}_{\mu\nu}) \tag{15}$$

and

$$P^z_{\mu\nu} = D^{\alpha\alpha}_{\mu\nu} - D^{\beta\beta}_{\mu\nu} \tag{16}$$

In eq 13, $\mathcal{W}^A_{\mu\nu}$ is defined from the Löwdin partitioning as

$$\mathcal{W}^A_{\mu\nu} = \sum_{\lambda\in A} (\mathbf{S}^{1/2})_{\mu\lambda}(\mathbf{S}^{1/2})_{\lambda\nu} \tag{17}$$

where $\mathbf{S}$ is the AO overlap matrix. For each atom A for which the local magnetization $\mathbf{m}_A$ is to be constrained in a direction $\mathbf{e}_A$, an additional term $\mathbf{h}_A$ is included in $\mathbf{H}_{KS}$ such that

$$\mathbf{h}^A = \mathcal{W}^A\boldsymbol{\lambda}_A\cdot(\boldsymbol{\sigma}\times\mathbf{e}_A) \tag{18}$$

where $\mathbf{e}_A$ is a unit vector to which $\mathbf{m}_A$ is constraint to be parallel to and $\boldsymbol{\lambda}_A$ is a Lagrange multiplier vector. The initial state for the dynamics simulation is then generated by solving the KS equations self-consistently while optimizing $\boldsymbol{\lambda}_A$ at each cycle so that $\mathbf{m}_A \times \mathbf{e}_A = 0$.

Having set the initial conditions, the total propagation time is divided uniformly in small propagation steps dt. The time step is reduced upon failure of idempotency and trace tests of the density matrix (RMS error of 10^{-6}), which are performed at each step during the dynamics. In our experience, the largest time step and total propagation time for which the idempotency and trace conditions are satisfied moderately depend on the basis set employed. We also check for convergence during the matrix exponentiation (RMS of 10^{-14} in the last term in the series) to make sure that the error is below a desired threshold.

For our benchmark calculations we consider two systems: The linear H−He−H molecule with an H−He distance of 1.6 Å and the [Cu(bpy)(H_2O)(NO_3)2(μ-C_2O_4)] (BISDOW) complex with the structure taken from the open-shell database of Valero et al.[63] We utilize the PBE functional[64,65] within the adiabatic approximation in conjunction with the 6-31G* basis for the H−He−H molecule, and the 6-31G* for Cu and the 6-

DOI: 10.1021/acs.jctc.5b00494
J. Chem. Theory Comput. 2015, 11, 3661−3668

31G basis for the other elements of the BISDOW complex. The total propagation times and time steps employed were 25,000 au and 0.5 au (605 fs and 12.1 as) for H−He−H, and 2,000 a.u and 0.2 au (48.4 fs and 4.84 as) for the BISDOW complex, respectively. The total propagation time for H−He−H was chosen so that it contains approximately 10 precession cycles. The propagation for the BISDOW complex is more computationally demanding than for H−He−H and hence we set the total propagation time to approximately one full precession cycle of the Cu magnetization.

To analyze the dynamics we calculated and recorded the local magnetic moments of each atom at every time step. For this purpose we use the well-known Hirshfeld partitioning of the electron density and magnetization[66,67] which shows low variation with respect to basis set choice for magnetization analyses.[68] Within this scheme atomic weight functions $w_A(\mathbf{r})$ are calculated as

$$w_A(\mathbf{r}) = \frac{n_A^0(\mathbf{r} - \mathbf{R}_A)}{\sum_{B \neq A} n_B^0(\mathbf{r} - \mathbf{R}_B)} \tag{19}$$

where n_A^0 and n_B^0 are the spherically symmetric atomic densities of the isolated atoms and $\mathbf{R}_A$ and $\mathbf{R}_B$ are the nuclear positions. Using this weight function, the Cartesian components of the atomic magnetic moments can be evaluated as

$$m_{A\,i} = \int d^3r\; w_A(\mathbf{r}) \sum_{\mu\nu} P_{\mu\nu}^i \phi_\mu(\mathbf{r}) \phi_\nu(\mathbf{r}) \tag{20}$$

with $i = x, y, z$.

The methodology described above was implemented and tested in an in-house development version of the Gaussian suite of programs.[40] In all calculations no symmetry constraints ("nosymm" keyword) were used, and the numerical integration was performed using a pruned grid of 99 radial shells and 590 angular points per atomic shell ("grid=ultrafine"). No relativistic effects (scalar or spin−orbit) were included in the calculations.

4. RESULTS AND DISCUSSION

We first look into the dynamics of the linear H−He−H molecule that has been employed as a simple model system to assess different methods for the calculation of magnetic exchange couplings due to its magnetic behavior, which follows very closely that of a Heisenberg−Dirac-Van Vleck (HDVV) Hamiltonian.[69,70] The dynamics was initiated from an off-equilibrium state in which the magnetization at each H atom was constrained to form an angle α from the $+z$ axis using the methodology describe above (see Figure 1). Monitoring the local magnetization at each H atom, $\mathbf{m}_H = \langle \mathbf{S} \rangle_H$, during the time evolution we observe the expected classical spin precession of a HDVV dimer, where each $\mathbf{m}_H$ precesses harmonically around the total spin $\mathbf{S}_T$ (see Figure 2). This suggests that the dynamical behavior of a HDVV dimer is fully captured by our TDDFT simulations. In Figure 1 we show a snapshot of this spin precession from our TDDFT GGA simulation. Our results show that with the simple adiabatic GGA approximation we recover the HDVV behavior for the low-frequency dynamics of a spin dimer systems and are consistent with the observation of Stamenova and Sanvito for the same system using the LSDA and a different spin population method and initial conditions.[38] These results provide a justification for the use of the HDVV model for these type of systems from a dynamic point of view.

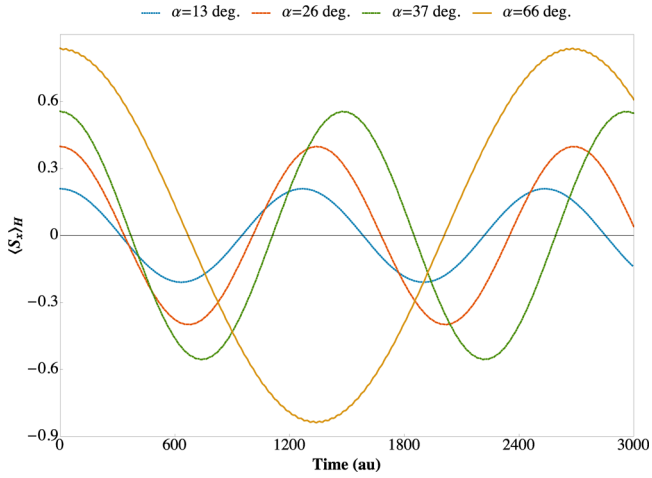

Figure 2. Time-evolution of the x-component of the magnetization of the H-He-H system (see Figure 1) at each H atom, $\langle S_x \rangle_H$, for simulations starting from different out-of-equilibrium configurations.

To further validate our approach it is useful to attempt a more quantitative analysis of the exchange interactions obtained from stationary DFT and from the dynamic simulations. From the HDVV Hamiltonian for a spin dimer

$$\hat{H}_{HDVV} = -J\hat{\mathbf{S}}_1 \cdot \hat{\mathbf{S}}_2 \tag{21}$$

where $\hat{\mathbf{S}}_1$ and $\hat{\mathbf{S}}_2$ represent the spin operators of two localized particles of spin S_1 and S_2, respectively, the exchange coupling constant J can be obtained from the energy difference between the high-spin (HS) $|\uparrow\uparrow\rangle$ and broken-symmetry (BS) $|\uparrow\downarrow\rangle$ states as

$$J = \frac{\Delta E}{2S_1S_2} \tag{22}$$

where $\Delta E = \langle \uparrow\downarrow | \hat{H}_{HDVV} | \uparrow\downarrow \rangle - \langle \uparrow\uparrow | \hat{H}_{HDVV} | \uparrow\uparrow \rangle$. Assuming that the HS and BS states can be accurately represented by KS theory, this provides a route for the calculation of the coupling constants from stationary DFT calculations.[71−77] Alternatively, we can estimate the J coupling from our TDDFT simulations. To this end, it is convenient to consider the classical interaction Hamiltonian between two magnetic moments $\mathbf{S}_1$ and $\mathbf{S}_2$

$$H_C = -J\mathbf{S}_1 \cdot \mathbf{S}_2 \tag{23}$$

The equations of motion can be obtained from the Poisson brackets of $\mathbf{S}_1$ and $\mathbf{S}_2$ with H_C

$$\frac{d\mathbf{S}_1}{dt} = J\mathbf{S}_1 \times \mathbf{S}_2 \tag{24}$$

and

$$\frac{d\mathbf{S}_2}{dt} = J\mathbf{S}_2 \times \mathbf{S}_1 \tag{25}$$

which leads to the well-known harmonic precession of $\mathbf{S}_1$ and $\mathbf{S}_2$ around a constant $\mathbf{S}_T = \mathbf{S}_1 + \mathbf{S}_2$ with frequency $\omega = J\,|\mathbf{S}_T|$. From the dynamic TDDFT simulation, J can therefore be obtained from the precession frequency of the spin dimer and the total (constant) magnetic moment. The frequency ω in this case corresponds to the lowest frequency of the precession and can be obtained by either fitting the local magnetic moments (calculated in our case using the Hirshfeld partitioning

DOI: 10.1021/acs.jctc.5b00494
J. Chem. Theory Comput. 2015, 11, 3661−3668

described in Section 3) for the first few periods with an harmonic function, or by Fourier-transforming the local magnetic moments dynamics for a sufficiently long simulation covering several precession periods. Although both approaches seem somewhat impractical for the sole purpose of obtaining the J coupling, they provide a practical venue for analyzing magnetic phenomena from TDDFT. The sign of the coupling constant $J = \omega|\mathbf{S}_T|$ can be determined from the precession direction, being positive for clockwise precession. The precession frequency depends on the initial off-equilibrium configuration, which also determines $|\mathbf{S}_T|$. In Figure 2 we show the time-evolution of $\langle S_x\rangle_H$ for simulations starting from different off-equilibrium configurations. From these simulations we fit the frequencies and calculate the corresponding J couplings in Table 1. The variation of J with the starting

Table 1. Calculated H−H Magnetic Exchange Couplings J (meV) in H−He−H from TDDFT Dynamic Simulations from Different Starting Configurations[a]

α	S_T	ω	$J = -\omega/S_T$
13	0.97	496	−138.5
26	0.90	468	−141.3
37	0.80	424	−145.0
66	0.41	235	−156.2

[a]Each starting configuration corresponds to an off-equilibrium state with the magnetization at each H atom forming an angle α (deg.) with the $+z$ axis in opposite directions (in the x−z plane). Frequencies ω (au/10^5) were obtained by fitting the time-evolution of the first four cycles with a harmonic function. The exchange coupling value calculated from the total (spin collinear) energy differences is J = −148.4 meV. S_T values are in au.

configuration can be attributed to the ambiguous definition of the local magnetization and is consistent with the results of Stamenova and Sanvito[38] and with our previous results employing the second derivative of the KS energy with respect to the constraint angle.[78] In particular, we have found in ref 78 a smaller (negative) J value for the HS configuration (α = 0) and a larger (negative) value for the BS solution (α = 90 deg) with differences of ca. 6%. It should be noted that the J coupling extracted from the dynamic simulation is expected to depend on the particular choice of spin population, as demonstrated in ref 38.

We have also tested our TDDFT code in the bimetallic Cu_2 complex BISDOW (see Figure 3). This complex consists of two Cu(II) centrosymmetric neutral atoms placed in a strongly elongated octahedral environment, surrounded by two N atoms of a bipyridine molecule and two O atoms of the bridging oxalate group in the equatorial plane. The two Cu(II) centers are coupled through the oxalate group leading to an experimental J coupling of −47 meV (−382 cm^{-1}) as determined by variable temperature magnetic susceptibility measurements.[79] As in the linear H−He−H case, the magnetization dynamics in the BISDOW complex also follows closely the behavior of a classical HDVV system dominated by a harmonic precession at the two Cu centers around the total molecular magnetization.

In Figure 4 we show $\langle S_x\rangle_{Cu}$ for one of the Cu atoms as a function of time. By fitting $\langle S_x\rangle_{Cu}$ with a harmonic function we calculate the J coupling from TDDFT to be −201.2 meV, which is in line with the J coupling obtained from energy differences of −226.7 meV. These couplings are larger in

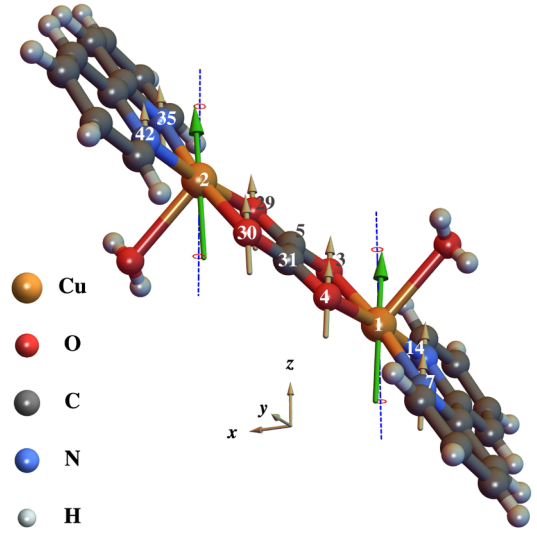

Figure 3. Representation of the magnetization precession for Cu atoms and their ligands in the BISDOW complex. The arrows represent the magnetization direction evaluated as described in the text and are not to scale.

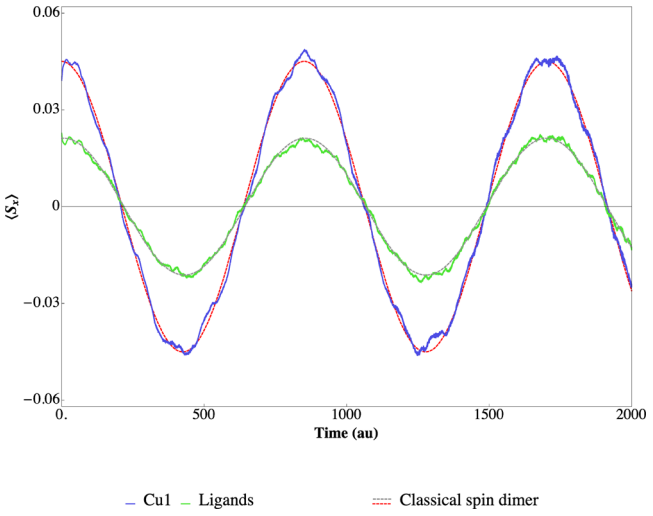

Figure 4. $\langle S_x\rangle$ for the Cu1 atom (full blue line) and its ligands (full green line, $\langle S_x\rangle$ summed over C2, C4, N7, and N14 atoms in Figure 3) as a function of time from the TDDFT simulation. A best harmonic fit to a classical spin dimer is included for comparison (dotted lines).

magnitude than the experimental value (−47 meV) due to the well known tendency of GGAs to delocalize the magnetization. It should be noted that other families of exchange-correlation density functional approximations, such as hybrid functionals, often yield J in better agreement with experimental values.[80−84] In complexes such as BISDOW, the spin-density at the transition metal atoms typically delocalizes into the neighboring ligands, and this is expected to influence the dynamics. In Figure 4 we show $\langle S_x\rangle$ summed over all the ligands of Cu1 (C2, C4, N7, and N14 atoms in Figure 3). The magnetization at the ligands precesses mostly parallel and at the same frequency as that of the Cu1 center with some high-frequency features of small amplitude on top of the main low-frequency harmonic component. We interpret these features as a result of the delocalization of the spin-density into the ligands (Figure 3), which causes small deviations from the idealized HDVV behavior.

DOI: 10.1021/acs.jctc.5b00494
J. Chem. Theory Comput. 2015, 11, 3661−3668

5. CONCLUDING REMARKS

We have presented a computational approach for the simultaneous dynamics of charge and magnetization in molecular systems in the context of the TDDFT formalism. Our method employs a second-order Magnus propagator with the efficient predictor-corrector scheme proposed by Cheng et al.[46] combined with a general extension of noncollinear ground-state spin DFT proposed previously.[33] This results in a powerful computational tool to study problems where spin dynamics is relevant. We have tested this method to model the low-frequency spin dynamics of a H−He−H model. Our simulations employ a noncollinear extension of the GGA PBE functional and make use of constraints that precondition the local spin out of equilibrium to initiate the propagation. In line with the observations of Stamenova and Sanvito with the LSDA,[38] we find that the dynamics of the H−He−H molecule can be modeled by the simple classical magnetization precession of a Heisenberg−Dirac-van Vleck system. The dynamics is characterized by noncollinear $\langle \mathbf{S} \rangle$ at each hydrogen atom precessing about the total spin $\langle \mathbf{S}_T \rangle$. We have also analyzed the magnetization dynamics of the bimetallic complex $[Cu(bpy)(H_2O)(NO_3)2(\mu\text{-}C_2O_4)]$ (BISDOW), where $\langle \mathbf{S} \rangle$ at each Cu atom and its ligands precesses as a whole, similar to the H−He−H case, indicating that the main features of a HDVV Hamiltonian are recovered for this complex as well. In this case, however, the precession is not purely harmonic and high-frequency features of small amplitude appear on top of the main low-frequency harmonic component. We hypothesize that these features originate from the delocalization of the spin-density toward the ligands. In both cases, H−He−H and BISDOW, we were able to to extract magnetic exchange couplings from the low-frequency precession given by our TDDFT simulations and compare with good agreement to the traditional energy differences method.

■ ASSOCIATED CONTENT

Supporting Information

Raw data obtained from the simulations for H−He−H and BISDOW, and classical magnetization precession animations for visualization purposes. The Supporting Information is available free of charge on the ACS Publications website at DOI: 10.1021/acs.jctc.5b00494.

■ AUTHOR INFORMATION

Corresponding Author

*E-mail: juan.peralta@cmich.edu.

Notes

The authors declare no competing financial interest.

■ ACKNOWLEDGMENTS

The authors thank Roi Baer for helpful discussions. J.E.P. acknowledges support from the US Department of Energy Grant No. DE-FG02-10ER16203. Work at TAU was supported by the Israel Science Foundation under grant No. 1740/13, the Lise-Meitner Minerva Center for Computational Quantum Chemistry, and the Center for Nanoscience and Nanotechnology at Tel-Aviv University. G.E.S. acknowledges that this material is based upon work supported by the U.S. Department of Energy, Office of Science, Office of Basic Energy Sciences, Heavy Element Chemistry Program under Award Number DE-FG02-04ER15523. G.E.S. is a Welch Foundation Chair (C-0036).

■ REFERENCES

(1) Runge, E.; Gross, E. K. U. Density-Functional Theory for Time-Dependent Systems. *Phys. Rev. Lett.* **1984**, *52*, 997.
(2) Petersilka, M.; Gossmann, U. J.; Gross, E. K. U. Excitation Energies from Time-Dependent Density-Functional Theory. *Phys. Rev. Lett.* **1996**, *76*, 1212−1215.
(3) Marques, M.; Gross, E. Time-dependent Density Functional Theory. *Annu. Rev. Phys. Chem.* **2004**, *55*, 427−455.
(4) Burke, K.; Werschnik, J.; Gross, E. K. U. Time-dependent Density Functional Theory: Past,Present, and Future. *J. Chem. Phys.* **2005**, *123*, 062206.
(5) Sugino, O.; Miyamoto, Y. In *Time-Dependent Density Functional Theory*; Marques, M. A., Ullrich, C. A., Nogueira, F., Rubio, A., Burke, K., Gross, E. K. U., Eds.; Lecture Notes in Physics; Springer: Berlin, Heidelberg, 2006; Vol. *706*, pp 407−420.
(6) Yabana, K.; Bertsch, G. F. Time-dependent Local-density Approximation in Real Time. *Phys. Rev. B: Condens. Matter Mater. Phys.* **1996**, *54*, 4484−4487.
(7) Tsolakidis, A.; Sánchez-Portal, D.; Martin, R. M. Calculation of the Optical Response of Atomic Clusters Using Time-dependent Density Functional Theory and Local Orbitals. *Phys. Rev. B: Condens. Matter Mater. Phys.* **2002**, *66*, 235416.
(8) Tsolakidis, A.; Kaxiras, E. A TDDFT Study of the Optical Response of DNA Bases, Base Pairs, and Their Tautomers in the Gas Phase. *J. Phys. Chem. A* **2005**, *109*, 2373−2380.
(9) Yabana, K.; Nakatsukasa, T.; Iwata, J.-I.; Bertsch, G. F. Real-time, real-space implementation of the linear response time-dependent density-functional theory. *Phys. Status Solidi B* **2006**, *243*, 1121−1138.
(10) Li, X.; Tully, J. C. Ab Initio Time-resolved Density Functional Theory for Lifetimes of Excited Adsorbate States at Metal Surfaces. *Chem. Phys. Lett.* **2007**, *439*, 199−203.
(11) Kubar, T.; Elstner, M. Coarse-Grained Time-Dependent Density Functional Simulation of Charge Transfer in Complex Systems: Application to Hole Transfer in DNA. *J. Phys. Chem. B* **2010**, *114*, 11221−11240.
(12) Reinhard, P.-G.; Suraud, E. In *Time-Dependent Density Functional Theory*; Marques, M. A., Ullrich, C. A., Nogueira, F., Rubio, A., Burke, K., Gross, E. K. U., Eds.; Lecture Notes in Physics; Springer: Berlin, Heidelberg, 2006; Vol. *706*, pp 391−406.
(13) Baer, R.; Seideman, T.; Ilani, S.; Neuhauser, D. Ab Initio Study of the Alternating Current Impedance of a Molecular Junction. *J. Chem. Phys.* **2004**, *120*, 3387−3396.
(14) Baer, R.; Neuhauser, D. Ab Initio Electrical Conductance of a Molecular Wire. *Int. J. Quantum Chem.* **2003**, *91*, 524−532.
(15) Di Ventra, M.; Lang, N. D. Transport in Nanoscale Conductors from First Principles. *Phys. Rev. B: Condens. Matter Mater. Phys.* **2001**, *65*, 045402.
(16) Di Ventra, M.; D'Agosta, R. Stochastic Time-Dependent Current-Density-Functional Theory. *Phys. Rev. Lett.* **2007**, *98*, 226403.
(17) Zelovich, T.; Kronik, L.; Hod, O. State Representation Approach for Atomistic Time-Dependent Transport Calculations in Molecular Junctions. *J. Chem. Theory Comput.* **2014**, *10*, 2927−2941.
(18) Prinz, G. A. Magnetoelectronics. *Science* **1998**, *282*, 1660−1663.
(19) Wolf, S. A.; Awschalom, D. D.; Buhrman, R. A.; Daughton, J. M.; von Molnár, S.; Roukes, M. L.; Chtchelkanova, A. Y.; Treger, D. M. Spintronics: A Spin-Based Electronics Vision for the Future. *Science* **2001**, *294*, 1488−1495.
(20) Zutic, I.; Fabian, J.; das Sarma, S. Spintronics: Fundamentals and Applications. *Rev. Mod. Phys.* **2004**, *76*, 323−410.
(21) Capelle, K.; Vignale, G.; Györffy, B. L. Spin Currents and Spin Dynamics in Time-Dependent Density-Functional Theory. *Phys. Rev. Lett.* **2001**, *87*, 206403.
(22) Sharma, S.; Dewhurst, J. K.; Ambrosch-Draxl, C.; Kurth, S.; Helbig, N.; Pittalis, S.; Shallcross, S.; Nordström, L.; Gross, E. K. U. First-Principles Approach to Noncollinear Magnetism: Towards Spin Dynamics. *Phys. Rev. Lett.* **2007**, *98*, 196405.
(23) Tsunoda, Y. Spin-density Wave in Cubic γ-Fe and γ-$Fe_{100-x}Co_x$ Precipitates in Cu. *J. Phys.: Condens. Matter* **1989**, *1*, 10427.

(24) Sjöstedt, E.; Nordström, L. Noncollinear Full-potential Studies of γ-Fe. *Phys. Rev. B: Condens. Matter Mater. Phys.* **2002**, *66*, 014447.
(25) Grohol, D.; Matan, K.; Cho, J.-H.; Lee, S.-H.; Lynn, J. W.; Nocera, D. G.; Lee, Y. S. Spin Chirality on a Two-dimensional Frustrated Lattice. *Nat. Mater.* **2005**, *4*, 323−328.
(26) Venturini, G.; Welter, R.; Ressouche, E.; Malaman, B. Neutron Diffraction Studies of $LaMn_2Ge_2$ and $LaMn_2Si_2$ Compounds: Evidence of Dominant Antiferromagnetic Components Within the Mn Planes. *J. Alloys Compd.* **1994**, *210*, 213−220.
(27) Uchida, M.; Onose, Y.; Matsui, Y.; Tokura, Y. Real-Space Observation of Helical Spin Order. *Science* **2006**, *311*, 359−361.
(28) Kübler, J.; Höck, K.-H.; Sticht, J.; Williams, A. R. Density Functional Theory of Non-collinear Magnetism. *J. Phys. F: Met. Phys.* **1988**, *18*, 469−483.
(29) Nordsröm, L.; Singh, D. J. Noncollinear Intra-atomic Magnetism. *Phys. Rev. Lett.* **1996**, *76*, 4420−4423.
(30) Oda, T.; Pasquarello, A.; Car, R. Fully Unconstrained Approach to Noncollinear Magnetism: Application to Small Fe Clusters. *Phys. Rev. Lett.* **1998**, *80*, 3622−3625.
(31) Yamanaka, S.; Yamaki, D.; Shigeta, Y.; Nagao, H.; Yoshioka, Y.; Suzuki, N.; Yamaguchi, K. Generalized Spin Density Functional Theory for Noncollinear Molecular Magnetism. *Int. J. Quantum Chem.* **2000**, *80*, 664−671.
(32) Kurz, Ph.; Förster, F.; Nordsröm, L.; Bihlmayer, G.; Blügel, S. Ab Initio Treatment of Noncollinear Magnets With the Full-potential Linearized Augmented Plane Wave Method. *Phys. Rev. B: Condens. Matter Mater. Phys.* **2004**, *69*, 024415.
(33) Peralta, J. E.; Scuseria, G. E.; Frisch, M. J. Noncollinear Magnetism in Density Functional Calculations. *Phys. Rev. B: Condens. Matter Mater. Phys.* **2007**, *75*, 125119.
(34) Wang, F.; Ziegler, T. Time-dependent Density Functional Theory Based on a Noncollinear Formulation of the Exchange-correlation Potential. *J. Chem. Phys.* **2004**, *121*, 12191−12196.
(35) Vahtras, O.; Rinkevicius, Z. General excitations in time-dependent density functional theory. *J. Chem. Phys.* **2007**, *126*, 114101.
(36) Li, Z.; Liu, W. Theoretical and Numerical Assessments of Spin-flip Time-dependent Density Functional Theory. *J. Chem. Phys.* **2012**, *136*, 024107.
(37) Ding, F.; Goings, J. J.; Frisch, M. J.; Li, X. Ab Initio Non-relativistic Spin Dynamics. *J. Chem. Phys.* **2014**, *141*, 214111.
(38) Stamenova, M.; Sanvito, S. Dynamical Exchange Interaction from Time-dependent Spin Density Functional Theory. *Phys. Rev. B: Condens. Matter Mater. Phys.* **2013**, *88*, 104423.
(39) Krieger, K.; Dewhurst, J. K.; Elliott, P.; Sharma, S.; Gross, E. K. U. Laser Induced Ultrafast Demagnetization: An *Ab-initio* Perspective, 2014. http://arxiv.org/abs/1406.6607v1 (accessed July 1, 2015).
(40) Frisch, M. J.; Trucks, G. W.; Schlegel, H. B.; Scuseria, G. E.; Robb, M. A.; Cheeseman, J. R.; Scalmani, G.; Barone, V.; Mennucci, B.; Petersson, G. A.; Nakatsuji, H.; Caricato, M.; Li, X.; Hratchian, H. P.; Izmaylov, A. F.; Bloino, J.; Zheng, G.; Sonnenberg, J. L.; Hada, M.; Ehara, M.; Toyota, K.; Fukuda, R.; Hasegawa, J.; Ishida, M.; Nakajima, T.; Honda, Y.; Kitao, O.; Nakai, H.; Vreven, T.; Montgomery, J. A., Jr.; Peralta, J. E.; Ogliaro, F.; Bearpark, M.; Heyd, J. J.; Brothers, E.; Kudin, K. N.; Staroverov, V. N.; Kobayashi, R.; Normand, J.; Raghavachari, K.; Rendell, A.; Burant, J. C.; Iyengar, S. S.; Tomasi, J.; Cossi, M.; Rega, N.; Millam, J. M.; Klene, M.; Knox, J. E.; Cross, J. B.; Bakken, V.; Adamo, C.; Jaramillo, J.; Gomperts, R.; Stratmann, R. E.; Yazyev, O.; Austin, A. J.; Cammi, R.; Pomelli, C.; Ochterski, J. W.; Martin, R. L.; Morokuma, K.; Zakrzewski, V. G.; Voth, G. A.; Salvador, P.; Dannenberg, J. J.; Dapprich, S.; Parandekar, P. V.; Mayhall, N. J.; Daniels, A. D.; Farkas, O.; Foresman, J. B.; Ortiz, J. V.; Cioslowski, J.; Fox, D. J. *Gaussian Development Version, Revision H.32*; Gaussian, Inc.: Wallingford, CT, 2009.
(41) Wijewardane, H. O.; Ullrich, C. A. Time-Dependent Kohn-Sham Theory with Memory. *Phys. Rev. Lett.* **2005**, *95*, 086401.
(42) Kurzweil, Y.; Baer, R. Generic Galilean-invariant Exchange-correlation Functionals With Quantum Memory. *Phys. Rev. B: Condens. Matter Mater. Phys.* **2005**, *72*, 035106.
(43) Kurzweil, Y.; Baer, R. Adapting Approximate-memory Potentials for Time-dependent Density Functional Theory. *Phys. Rev. B: Condens. Matter Mater. Phys.* **2008**, *77*, 085121.
(44) Magnus, W. On the Exponential Solution of Differential Equations for a Linear Operator. *Comm. Pure Appl. Math.* **1954**, *7*, 649−673.
(45) Castro, A.; Marques, M. A. L.; Rubio, A. Propagators for the Time-dependent Kohn-Sham Equations. *J. Chem. Phys.* **2004**, *121*, 3425−3433.
(46) Cheng, C.-L.; Evans, J. S.; Van Voorhis, T. Simulating Molecular Conductance Using Real-time Density Functional Theory. *Phys. Rev. B: Condens. Matter Mater. Phys.* **2006**, *74*, 155112.
(47) Lopata, K.; Govind, N. Modeling Fast Electron Dynamics with Real-Time Time-Dependent Density Functional Theory: Application to Small Molecules and Chromophores. *J. Chem. Theory Comput.* **2011**, *7*, 1344−1355.
(48) Moler, C.; Van Loan, C. Nineteen Dubious Ways to Compute the Exponential of a Matrix, Twenty-Five Years Later. *SIAM Rev.* **2003**, *45*, 3−49.
(49) Isborn, C. M.; Li, X. Singlet-Triplet Transitions in Real-Time Time-Dependent Hartree-Fock/Density Functional Theory. *J. Chem. Theory Comput.* **2009**, *5*, 2415−2419.
(50) Mejía-López, J.; Romero, A. H.; Garcia, M. E.; Morán-López, J. L. Noncollinear Magnetism, Spin Frustration, and Magnetic Nano-domains in Small Mn_n clusters. *Phys. Rev. B: Condens. Matter Mater. Phys.* **2006**, *74*, 140405.
(51) Mayer, M.; Krüger, S.; Rösch, N. A two-component Variant of the Douglas-Kroll Relativistic Linear Combination of Gaussian-type Orbitals Density-functional Method: Spin-orbit Effects in Atoms and Diatomics. *J. Chem. Phys.* **2001**, *115*, 4411−4423.
(52) Peralta, J. E.; Scuseria, G. E. Relativistic All-electron Two-component Self-consistent Density Functional Calculations Including One-electron Scalar and Spin-orbit Effects. *J. Chem. Phys.* **2004**, *120*, 5875−5881.
(53) Armbruster, M. K.; Weigend, F.; van Wüllen, C.; Klopper, W. Self-consistent Treatment of Spin-orbit Interactions With Efficient Hartree-Fock and Density Functional Methods. *Phys. Chem. Chem. Phys.* **2008**, *10*, 1748−1756.
(54) Kleinman, L. Density Functional for Noncollinear Magnetic Systems. *Phys. Rev. B: Condens. Matter Mater. Phys.* **1999**, *59*, 3314−3317.
(55) Scalmani, G.; Frisch, M. J. A New Approach to Noncollinear Spin Density Functional Theory beyond the Local Density Approximation. *J. Chem. Theory Comput.* **2012**, *8*, 2193−2196.
(56) Bulik, I. W.; Scalmani, G.; Frisch, M. J.; Scuseria, G. E. Noncollinear Density Functional Theory Having Proper Invariance and Local Torque Properties. *Phys. Rev. B: Condens. Matter Mater. Phys.* **2013**, *87*, 035117.
(57) Eich, F. G.; Pittalis, S.; Vignale, G. Transverse and Longitudinal Gradients of the Spin Magnetization in Spin-density-functional Theory. *Phys. Rev. B: Condens. Matter Mater. Phys.* **2013**, *88*, 245102.
(58) Liang, W.; Isborn, C. M.; Lindsay, A.; Li, X.; Smith, S. M.; Levis, R. J. Time-Dependent Density Functional Theory Calculations of Ehrenfest Dynamics of Laser Controlled Dissociation of NO+: Pulse Length and Sequential Multiple Single-Photon Processes. *J. Phys. Chem. A* **2010**, *114*, 6201−6206.
(59) Phillips, J. J.; Peralta, J. E. Magnetic Exchange Couplings from Constrained Density Functional Theory: An Efficient Approach Utilizing Analytic Derivatives. *J. Chem. Phys.* **2011**, *135*, 184108.
(60) Phillips, J. J.; Peralta, J. E. Towards the Blackbox Computation of Magnetic Exchange Coupling Parameters in Polynuclear Transition-metal Complexes: Theory, Implementation, and Application. *J. Chem. Phys.* **2013**, *138*, 174115.
(61) Clark, A. E.; Davidson, E. R. Local Spin. *J. Chem. Phys.* **2001**, *115*, 7382−7392.
(62) Herrmann, C.; Reiher, M.; Hess, B. Comparative Analysis of Local Spin Definitions. *J. Chem. Phys.* **2005**, *122*, 034102.
(63) Valero, R.; Costa, R.; de P. R. Moreira, I.; Truhlar, D. G.; Illas, F. Performance of the M06 Family of Exchange-correlation Functionals

DOI: 10.1021/acs.jctc.5b00494
J. Chem. Theory Comput. 2015, 11, 3661−3668

for Predicting Magnetic Coupling in Organic and Inorganic Molecules. *J. Chem. Phys.* **2008**, *128*, 114103.
(64) Perdew, J. P.; Burke, K.; Ernzerhof, M. Generalized Gradient Approximation Made Simple. *Phys. Rev. Lett.* **1996**, *77*, 3865−3868.
(65) Perdew, J. P.; Burke, K.; Ernzerhof, M. Generalized Gradient Approximation Made Simple (vol 77, pg 3865, 1996). *Phys. Rev. Lett.* **1997**, *78*, 1396−1396.
(66) Hirshfeld, F. Bonded-atom Fragments for Describing Molecular Charge-densities. *Theor. Chim. Acta* **1977**, *44*, 129−138.
(67) Bruhn, G.; Davidson, E.; Mayer, I.; Clark, A. Löwdin Population Analysis With and Without Rotational Invariance. *Int. J. Quantum Chem.* **2006**, *106*, 2065−2072.
(68) Phillips, J. J.; Hudspeth, M. A.; Browne, P. M., Jr.; Peralta, J. E. Basis Set Dependence of Atomic Spin Populations. *Chem. Phys. Lett.* **2010**, *495*, 146−150.
(69) Hart, J. R.; Rappe, A. K.; Gorun, S. M.; Upton, T. H. Estimation of magnetic exchange coupling constants in bridged dimer complexes. *J. Phys. Chem.* **1992**, *96*, 6264−6269.
(70) Ruiz, E.; Alvarez, S.; Cano, J.; Polo, V. About the calculation of exchange coupling constants using density-functional theory: The role of the self-interaction error. *J. Chem. Phys.* **2005**, *123*, 164110.
(71) Noodleman, L.; Case, D.; Aizman, A. Broken Symmetry Analysis of Spin Coupling in Iron Sulfur Clusters. *J. Am. Chem. Soc.* **1988**, *110*, 1001−1005.
(72) Caballol, R.; Castell, O.; Illas, F.; de P. R. Moreira, I.; Malrieu, J. Remarks on the Proper Use of the Broken Symmetry Approach to Magnetic Coupling. *J. Phys. Chem. A* **1997**, *101*, 7860−7866.
(73) Ruiz, E.; Cano, J.; Alvarez, S.; Alemany, P. Broken Symmetry Approach to Calculation of Exchange Coupling Constants for Homobinuclear and Heterobinuclear Transition Metal Complexes. *J. Comput. Chem.* **1999**, *20*, 1391−1400.
(74) Davidson, E. R.; Clark, A. E. Model Molecular Magnets. *J. Phys. Chem. A* **2002**, *106*, 7456−7461.
(75) Dai, D.; Whangbo, M.-H. Spin Exchange Interactions of a Spin Dimer: Analysis of Broken-symmetry Spin States in Terms of the Eigenstates of Heisenberg and Ising Spin Hamiltonians. *J. Chem. Phys.* **2003**, *118*, 29−39.
(76) Illas, F.; de P. R. Moreira, I.; Bofill, J.; Filatov, M. Extent and limitations of density-functional theory in describing magnetic systems. *Phys. Rev. B: Condens. Matter Mater. Phys.* **2004**, *70*, 132414.
(77) Rudra, I.; Wu, Q.; van Voorhis, T. Predicting Exchange Coupling Constants in Frustrated Molecular Magnets Using Density Functional Theory. *Inorg. Chem.* **2007**, *46*, 10539−10548.
(78) Peralta, J. E.; Barone, V. Magnetic Exchange Couplings from Noncollinear Spin Density Functional Perturbation Theory. *J. Chem. Phys.* **2008**, *129*, 194107.
(79) Castillo, O.; Muga, I.; Luque, A.; Gutierrez-Zorrilla, J. M.; Sertucha, J.; Vitoria, P.; Roman, P. Synthesis, Chemical Characterization, X-ray Crystal Structure and Magnetic Properties of Oxalato-bridged Copper(II) Binuclear Complexes With 2,2′-bipyridine and Diethylenetriamine as Peripheral Ligands. *Polyhedron* **1999**, *18*, 1235−1245.
(80) Martin, R. L.; Illas, F. Antiferromagnetic Exchange Interactions from Hybrid Density Functional Theory. *Phys. Rev. Lett.* **1997**, *79*, 1539−1542.
(81) Peralta, J. E.; Melo, J. I. Magnetic Exchange Couplings with Range-Separated Hybrid Density Functionals. *J. Chem. Theory Comput.* **2010**, *6*, 1894−1899.
(82) Schwabe, T.; Grimme, S. Calculation of Magnetic Couplings with Double-Hybrid Density Functionals. *J. Phys. Chem. Lett.* **2010**, *1*, 1201−1204.
(83) Rivero, P.; de P. R. Moreira, I.; Scuseria, G. E.; Illas, F. Description of magnetic interactions in strongly correlated solids via range-separated hybrid functionals. *Phys. Rev. B: Condens. Matter Mater. Phys.* **2009**, *79*, 245129.
(84) Phillips, J. J.; Peralta, J. E.; Janesko, B. G. Magnetic Exchange Couplings Evaluated with Rung 3.5 Density Functionals. *J. Chem. Phys.* **2011**, *134*, 214101.

DOI: 10.1021/acs.jctc.5b00494
J. Chem. Theory Comput. 2015, 11, 3661−3668